Original Research

Study on the Hydrochemical Characteristics and Environmental Background Values of Shallow Groundwater in the Qian'an Basin of Tangshan City, China

Xue Xia^{1, 2, 3}, Zhihui Qu^{1, 2, 30}*, Haowei Yuan⁴, Zhiqiang Gong⁵, Sihui Shao⁵, Huimin Kong^{1, 2, 3}, Biao Yu^{1, 2, 3}

¹Institute of Disaster Prevention, Sanhe 065201, China

²Hebei Key Laboratory of Resource and Environmental Disaster Mechanism and Risk Monitoring, Sanhe 065201, China

³Beijing Disaster Prevention Technology Co., Ltd, Beijing 101199, China

⁴CECEP DADI (Hangzhou) Envrionment Remediation Co., Ltd, Beijing, China

⁵Hebei Geological Environment Monitoring Institute, Shijiazhuang 050021, China

Received: 22 April 2025 Accepted: 13 September 2025

Abstract

This study is based on 63 sets of groundwater samples from the Qian'an Basin to calculate the environmental background values of groundwater, focusing on total dissolved solids (TDS), total hardness, and NO₃. Mathematical statistical methods were employed to identify and remove outliers. Ion correlation analysis and ratio plots were also used to investigate the chemical composition, formation mechanisms, and background values of the groundwater while analyzing the spatial distribution characteristics of these background values.

The research results showed that the dominant cations in the groundwater were Ca²⁺, followed by Mg²⁺, while the main anions were HCO₃ and SO₄²⁻. The hydrochemical types were classified as HCO₃-Ca·Mg and HCO₃SO₄-Ca·Mg, indicating that the dissolution of carbonate rocks played a dominant role in controlling the groundwater chemistry. The background value thresholds of total dissolved solids (TDS), total hardness, and NO₃ were calculated to be 162-729.95 mg/L, 122.05-508.55 mg/L, and 0.002-32.62 mg/L. The background values of TDS and total hardness showed no significant spatial variation overall. In contrast, the background values for NO₃ were higher and exhibited clear spatial variability, indicating that human activities influenced the groundwater. The study identified the hydrochemical and environmental background characteristics of shallow groundwater in the Qian'an Basin, deepening the understanding of the groundwater quality formation

°ORCID iD: 0000-0002-9053-4692

^{*}e-mail: qzh-19831001@163.com

and evolution mechanisms in the region compared to previous studies and providing important support for the sustainable development of regional groundwater.

Keywords: Qian'an basin, groundwater environmental background values, shallow groundwater, hydrochemical characteristics

Introduction

Groundwater is an important freshwater resource, and the formation of groundwater chemistry can be affected by a combination of natural factors and human activities [1]. However, the deterioration of groundwater quality that may result from natural processes and human activities poses a potential threat to human health and the environment [2, 3]; therefore, accurately identifying groundwater background values and revealing hydrochemical characteristics are essential for groundwater pollution assessment and environmental protection. Groundwater environmental background values are the characteristic values of the original chemical composition of the groundwater environment itself in its natural state without the influence of human activities [4-6]. Meanwhile, due to the mobility of groundwater and uneven distribution of waterbearing rock groups, different areas of groundwater recharge, runoff, and discharge, and differences in the intensity of water-rock interactions, the natural chemical components of groundwater have variations in certain spatial and temporal scales [7-9]. Hence, the groundwater environmental background value is a range value with spatial and temporal variability rather than a fixed value [10].

With the improvement of groundwater quality management requirements, scholars have gradually developed multi-dimensional and multi-scale technical paths in the research of background value calculation and recognition. Gianluigi Busico et al. [11] applied the well-known Gaussian Sequence Simulation Algorithm (SGS) to calculate and map the spatial distribution of background values such as NO, in groundwater. SGS retains the spatial properties of the variables compared to the traditional kriging interpolation method, which enables better prediction of the unknown space; Chu et al. [12] applied a random forest model to effectively identify TDS anomalies. However, although the random forest model can accurately detect high and low anomalies compared to traditional hydrochemical approaches, the underlying causes of these anomalies still require further analysis using additional methods; Awawdeh et al. [13] utilized a biphasic approach with an artificial neural network to successfully reduce the GRACE data to 4 km resolution, which combined the water level and its posterior data to achieve an accurate prediction of the groundwater level and provided an effective way to predict the accuracy of the background value identification and groundwater dynamics in the future.

Due to its topography, geographical location, and the influence of highly developed industrial and intensive agricultural activities, the water resources in Qian'an City are unevenly distributed in both time and space. The insufficient amount of groundwater resources [14] and the increasing contradiction between the supply and demand of water resources have led to the longterm overexploitation of groundwater in the study area of this paper, which has induced prominent problems of groundwater pollution and other systemic risks. Existing studies mainly focus on the evaluation and regulation of groundwater resources in Qian'an City, iron ore genesis [15], and the analysis of the current status of pollution in mining areas [16, 17]. Yang et al [18] carried out numerical simulation and water resource evaluation, and proposed a rational utilization scheme for long-term groundwater exploitation in Qian'an City; Xu et al [19] further established a numerical model of the groundwater system in the Qian'an Basin by combining the regional hydrogeological conditions, analyzed the regulation mechanism of surface water and groundwater, and provided countermeasures to support the realization of the sustainable utilization of groundwater resources; Meng et al [20] evaluated the groundwater in the mining area on the west side of the middle and lower reaches of the Luanhe River and pointed out that non-metallic pollution indicators, such as NO, and ammonia nitrogen, have a more significant impact on the quality of groundwater. However, there is still a lack of research on the natural chemical composition, formation mechanism, and distribution of groundwater in the Oian'an Basin.

To grasp the current status of the groundwater environment in Qian'an Basin, this paper, based on 63 sets of shallow groundwater data obtained in Qian'an Basin, adopted the mathematical and statistical method to determine groundwater environmental background values, used the Piper diagram, Gibbs diagram, and ionic proportion coefficient method in combination with the hydrogeological conditions to explore the hydrochemical characteristics of the groundwater and the evolution and formation of the groundwater components, and analyzed the spatial distribution characteristics and causes of the indicators of total dissolved solids (TDS), total hardness (TH), and NO₃ indicators in the basin. Different from previous studies that mainly focused on the evaluation of groundwater resources, mining regulation, or mining area pollution identification, this study is the first to carry out a comprehensive survey of background value identification, hydrochemical evolution characteristics, and spatial distribution in the Qian'an Basin to provide theoretical support for the sustainable use of groundwater resources and environmental protection in the Qian'an Basin.

Geological Setting

The Qian'an Basin, located in Qian'an City, Hebei Province, China, is a mountain-intermontane alluvial—pluvial basin whose formation and evolution are governed by the regional tectonic framework. The basin exhibits a north-high, south-low, and west-high, east-low topography, transitioning from low mountain hills to alluvial plains. The basin boundaries are controlled by NW-SE trending faults and a southwestwardly inclined "C"-shaped arcuate fold belt. These tectonic structures not only define the basin's morphology but also influence sediment distribution and groundwater flow direction.

The stratigraphy of the study area is primarily Archean basement composed of rocks, Mesoproterozoic Jixian and Changcheng Systems, and Quaternary deposits of the Cenozoic. The lithological characteristics of these different strata have distinct impacts on the groundwater system. The Archean rocks are mainly exposed around the periphery of the study area. They are dominated by metamorphic rocks such as mafic granulites, gneisses, and biotite-bearing metamorphic rocks, forming the dense basement of the basin. The Jixian and Changcheng Systems of the Mesoproterozoic are primarily exposed in the southwestern part of the basin and consist mainly of sedimentary rocks such as banded chert-bearing dolomites, quartz sandstones, and dolomitic limestones. The dissolution of carbonate rocks like dolostone releases substantial amounts of HCO3, Ca2+, and Mg2+ ions during weathering, which are important sources of the groundwater's chemical composition.

The groundwater in the study area is shallow, and the main aquifer is composed of Quaternary alluvial gravel. The aquifer thickness ranges from 8~20 m, and the aquifer lithology is dolomite. The region has the Luanhe River flowing in from the northwest and bending to flow out to the southeast, serving as the main recharge source for the Quaternary aquifer. The groundwater in the region is mainly composed of bedrock fracture water and Quaternary loose rock pore water, with bedrock fracture water distributed along the edges of the basin. Tectonic fractures control the water yield. The Quaternary unconsolidated pore water is primarily found in the floodplain of the Luanhe River and the first and second terraces. The mines controlled by the overturned anticline and faults are distributed along the outer edge of the basin. The natural weathering of the ore bodies and mining activities can increase the concentrations of ions such as Fe²⁺ and SO₄²⁻, which, through surface runoff and infiltration, enter the aquifer and have a cumulative effect on the hydrochemical composition of the groundwater. The study area and sampling points are shown in Fig. 1.

Materials and Methods

Sample Collection and Analysis

The sampling in this study focused on shallow groundwater, aiming to meet the precision requirements of hydrogeological investigations with a minimum sample size of 50 points at a scale of 1:100,000. A total of 63 groups of samples were collected and tested for 44 indicators, primarily focusing on exploring three key parameters: TH, TDS, and NO, .

The pH was measured using the glass electrode method. TDS was determined by the gravimetric method at 105°C. TH was analyzed using inductively coupled plasma atomic emission spectrometry (ICP-AES). Chemical oxygen demand (COD, represented as oxygen consumption) was measured using the acid potassium permanganate method. Major cations (Na⁺, K⁺, Ca²⁺, and Mg²⁺) and anions (Cl⁻, SO₄²⁻) were determined by ion chromatography (IC). Bicarbonate (HCO₃⁻) and carbonate (CO₃²⁻) concentrations were determined by acid-base titration.

Background Value Study Methodology

(1) Identification and removal of outliers

The study used mathematical statistics methods for outlier identification and rejection. The sample data needs to conform to a normal distribution after undergoing a normality test and normality transformation to identify outliers.

After completing the normality test, outliers were eliminated for macro components (K⁺, Ca²⁺, Na⁺, Mg²⁺, HCO₃, CO₃², SO₄², and Cl and composite indicators (pH, TDS, TH, and oxygen consumption) using the Piper diagram for sample data that conformed to a normal distribution. The diamond-shaped area of the Piper diagram was converted into two-dimensional coordinates. Then, the Mahalanobis distance formula (1) was used to calculate Da^2 for each sample's data points. The mean \pm 3SD (SD = standard deviation) of all the Da^2s was used as the critical distance (Di^2) . By comparing the magnitude of Di^2 with Da^2 , water chemistry anomalies were determined, and any samples with Da^2 values exceeding Di^2 were eliminated. The above steps were repeated until the Da^2 of all remaining samples was less than the critical distance Di². Outliers were subsequently identified and rejected using the Grubbs test.

Formula:

$$Da^{2} = (X - \overline{X})S^{-1}(X - \overline{X})^{T}$$
(1)

X – Coordinate values of the array;

 \bar{X} – Average of array coordinate values;

 S^{-1} – Inverse covariance matrix;

Da – Mahalanobis distance.

Depending on the number of remaining samples, the Grubbs test (sample size≤100) or the 3σ criterion

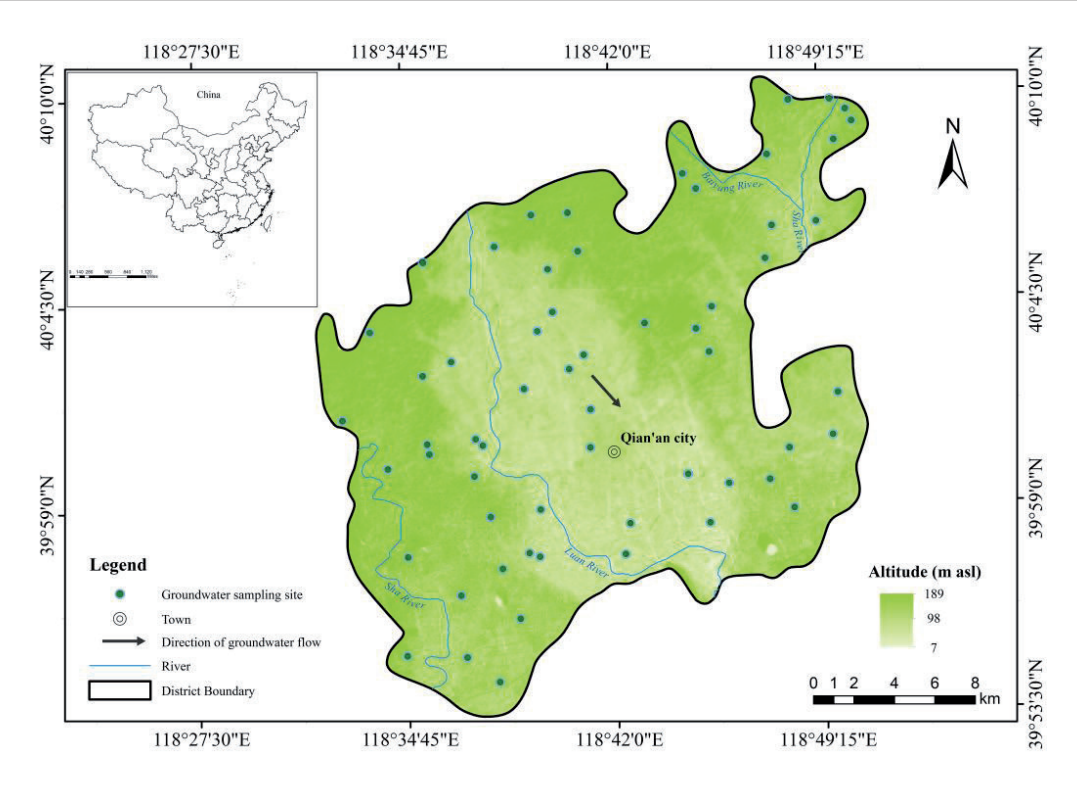


Fig. 1. Location map of the study area and groundwater sampling sites in Qian'an Basin.

(sample size > 100) was selected for outlier identification and removal.

If the NO_3^- in the study area presents surface contamination, the conventional method cannot identify the abnormal value. After replacing the undetected NO_3^- data in the sample data with the 1/2 detection limit, the data with the NO_3^- concentration > 10 mg/L can be directly regarded as abnormal data.

(2) Determination of background values

The cumulative frequency of individual components was statistically analyzed using SPSS, and the concentration corresponding to a cumulative frequency of 95% was taken as the upper limit of the background value. The background values for the groundwater environment are shown in Table 1.

Analytical Method

The flowchart of this study is shown in Fig. 2. After completing the calculation of background values, the Piper trilinear diagram was drawn to characterize the hydrochemical type of groundwater in the study area, and the Gibbs diagram was used to determine the formation mechanism and evolutionary characteristics of the hydrochemical composition of groundwater. Ion correlation analysis was used to determine the consistency and similarity of ion sources in the groundwater of the study area, and the ion proportion coefficient method was applied to analyze the possible mineral sources of the chemical components of the groundwater.

Results and Discussion

Hydrochemical Characteristics

Table 2 presents the statistical results of the main components of groundwater in the study area. The pH values of groundwater ranged from 6.60 to 8.50, with a mean value of 7.51, and its coefficient of variation was 5.16%. The mean value of regional TDS was 454.952 mg/L,

Table 1. Calculation results of background values of groundwater in the study area (mg/L).

Parameters	Valid sample	Mean	MAD	Std.Dev	Variance	Min	Max	Background range		C
								Lower limit	Upper limit	Coefficients of variation
TH	58	298.775862	307.0.	96.727696	9356.247	92	527	122.05	508.55	32.37%
TDS	58	401.327586	384.50	135.079105	18246.364	127	780	162	729.95	33.66%
NO ₃	57	11.439877	8.60	9.255963	85.673	0.002	38.7	0.002	32.62	80.91%

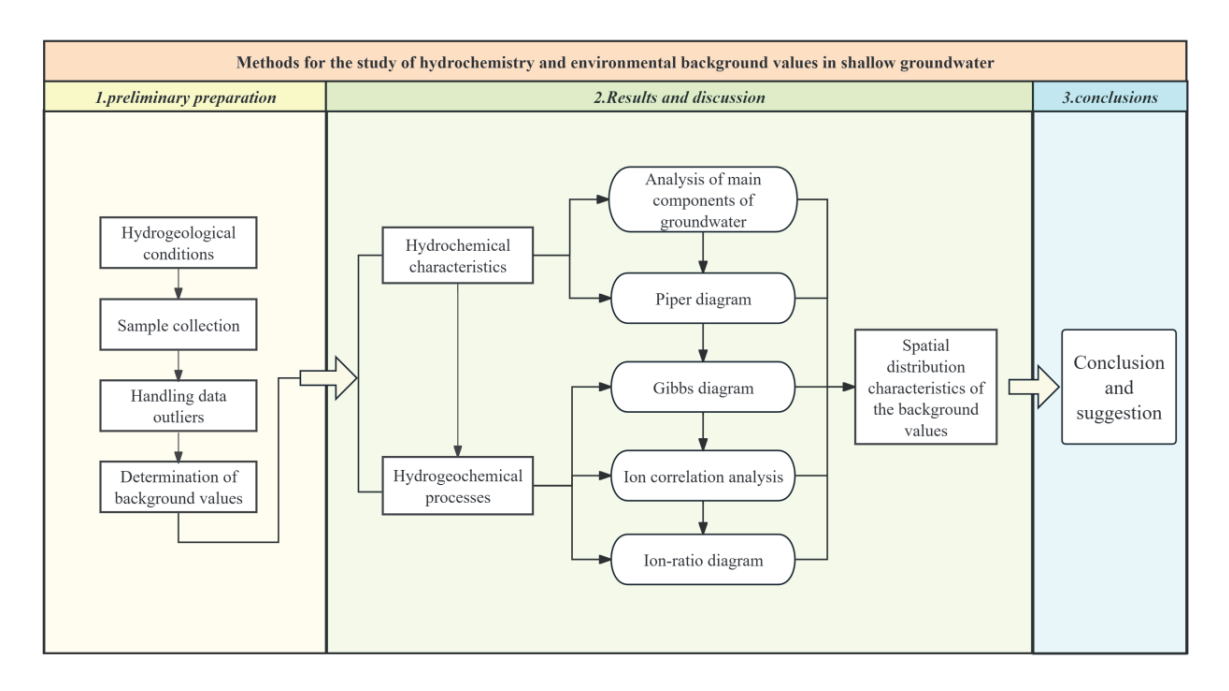


Fig. 2. Flowchart of the study steps.

and the coefficient of variation was 50.32%. The TH ranged from 92.00 to 851.00 mg/L, with a mean value of 333.53 mg/L, which was hard water. The concentrations of Mg²⁺, Ca²⁺, and Na⁺ ranged from 4.28 to 75.80 mg/L, 29.30 to 239 mg/L, and 8.03 to 78.40 mg/L, with average values of 24.872 mg/L, 91.841 mg/L, and 22.185 mg/L, respectively. The concentration of K⁺ in groundwater was relatively low, with a maximum value of 9.41 mg/L and an average of 1.967 mg/L. SO₄²⁻ showed the widest concentration range (9.21-645 mg/L), while HCO₃⁻ had the narrowest range (59-336 mg/L), with average values of 107.87 mg/L and 185.60 mg/L, respectively. The concentration of Cl⁻ ranged from 6.35 to 284 mg/L,

with a relatively large variation and an average of 36.64 mg/L. The main cation in the groundwater of the study area was Ca²⁺, and the main anion was HCO₃⁻.

Relatively low TDS values suggest that the aquifer has good runoff conditions, where the rapid water circulation process accelerates the renewal of water quality. The coefficients of variation of NO₃ and Cl were greater than one, showing very strong spatial variability; the coefficients of variation of the remaining anions and cations were all greater than 30%, indicating significant variability and dispersion in the spatial distribution; TH and TDS had smaller coefficients of variation, and the overall degree of variability was not significant within

Table 2. Main components of groundwater in the study area (mg/L).

Parameters	T 4 1 1		Concentration	C(1D	coefficients of	
	Total samples	Min	Max	Mean	Std.Dev	variation
Na ⁺	63	8.03	78.40	22.185	12.375549	55.78%
K^{+}	63	0.370	9.410	1.967	1.457548	74.09%
Ca ²⁺	63	29.30	239.0	91.841	38.596371	42.03%
Mg^{2+}	63	4.28	75.80	24.872	14.814068	59.56%
Cl-	63	6.35	284.00	36.642	41.230587	112.52%
SO ₄ ²⁻	63	9.21	645.00	107.872	87.587692	81.20%
HCO ₃	63	59.00	336.00	185.603	61.052738	32.89%
NO ₃	63	0.002	116.00	17.333	21.810082	125.83%
TH	63	92.00	851.00	331.571	148.707845	44.85%
TDS	63	127.00	1339.00	454.952	228.915073	50.32%
рН	63	6.60	8.50	7.510	0.387345	5.16%

the study area. Most of the groundwater with a TDS value less than 1000.00 mg/L belongs to fresh water.

Based on the calculated background values, a Piper trilinear diagram was constructed to graphically represent the major cations and anions in the water, directly illustrating the hydrochemical types. As shown in Fig. 3, the main hydrochemical types of groundwater in the study area are HCO3-Ca·Mg and HCO3·SO4-Ca·Mg. The distribution of water samples in the triangle of cations in the lower left corner was close to the Ca2+ and Mg2+ ends but away from the Na++K+ line. Ca2+ and Mg²⁺ were the dominant cations in the groundwater. Ca^{2+} was dominated by Ca^{2+} , followed by Mg^{2+} . The anion triangle in the lower right corner shows that the water sample was near the HCO₃-CO₃- end of the sample and that the anions were predominantly HCO₃, followed by SO₄². The TDS values were concentrated within the common range for shallow groundwater (100-1000 mg/L), indicating that the hydrochemical type of the groundwater was relatively stable and that ion concentrations were mainly controlled by carbonate dissolution.

Ca²⁺, Mg²⁺, and HCO₃⁻ were the major ions in the groundwater, primarily originating from the dissolution of dolomite and limestone. This suggested that the aquifer had favorable runoff conditions and a well-developed environment for carbonate dissolution [21], further enhancing the dissolution process. The groundwater circulation rate in the study area is slow, with well-developed water-rock interactions, and the dissolution of carbonate rocks influences the hydrochemical characteristics. Additionally, the surrounding dolomite aquifers, which are well-fractured,

allow groundwater to flow through the bedrock fractures and accumulate in the interior of the study area. This groundwater then interacts extensively with soluble CO₂, further enhancing the dissolution of carbonate rocks [22], leading to the gradual accumulation of HCO₃⁻ at the center of the region.

In the water samples, SO₄²⁻ was the second most abundant anion after HCO₃-, and the hydrochemical type was identified as HCO₃·SO₄-Ca·Mg. This was likely related to the rich mineral resources in the study area [23]. The Qian'an Basin is part of the eastern Hebei iron ore belt, which is characterized by sedimentary-metamorphic-type magnetite deposits, where pyrite commonly occurs alongside magnetite. Large-scale mining activities transformed the hydrogeochemical conditions from a relatively closed system to an open one. In this open environment, pyrite and other sulfurbearing compounds underwent a series of chemical reactions, leading to an increase in SO₄²⁻ concentrations [24].

Hydrogeochemical Processes

The Gibbs diagram is used to analyze and reveal the main controlling mechanisms responsible for the formation of chemical components in the water. The Gibbs diagram of groundwater in the study area is shown in Fig. 4. The ratio of Na⁺/(Na⁺+Ca²⁺) in Fig. 4a) ranged from 0.111 to 0.387, and the ratio of Cl⁻/(Cl⁻+HCO₃⁻) in Fig. 4b) was in the range of 0.055 to 0.352. The water samples were all located in the middle part of the rock weathering control end-member. They were relatively concentrated, indicating that water–rock

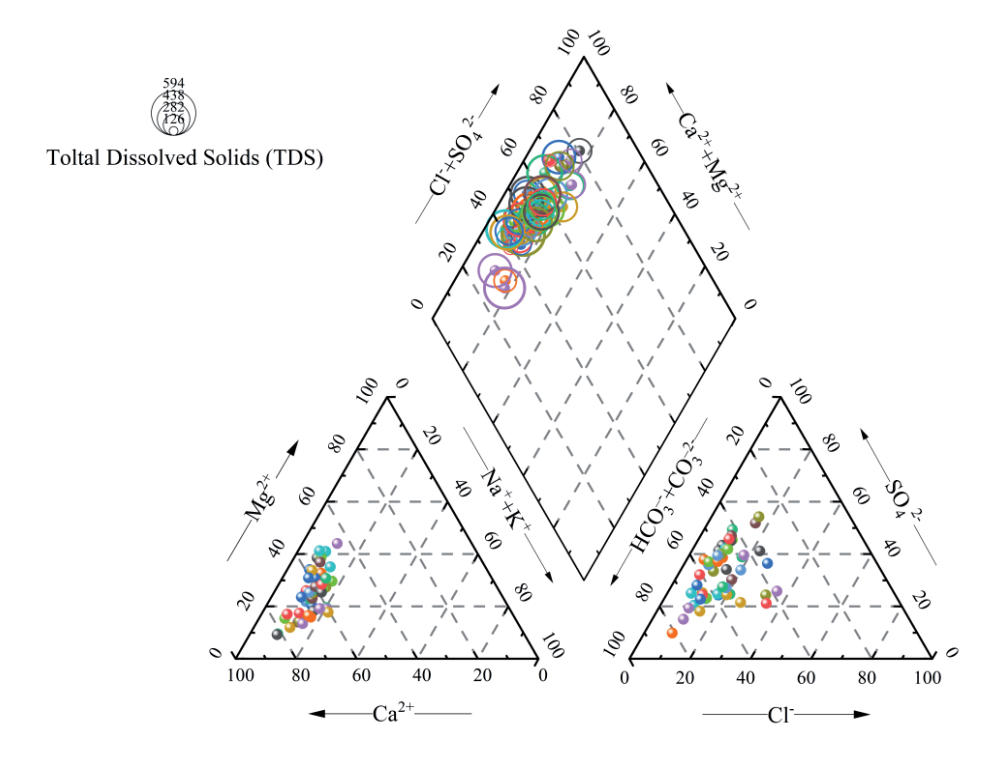
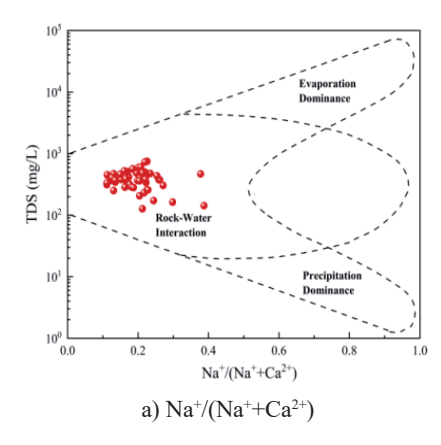


Fig. 3. Piper diagram of groundwater in the study area.





Rock-Water Interaction

Dominance

Precipitation
Dominance

10°

0.0 0.2 0.4 0.6 0.8 1.0

Cl'/(Cl+HCO₃)

b) Cl'/(Cl+HCO₃-)

interaction was the dominant mechanism controlling groundwater hydrochemistry in the study area.

The chemical composition of groundwater was formed over a long geological history during the groundwater flow process [25]. Carbonate rocks were widely distributed in the study area, and the dissolution of rock salt contributed significant amounts of Ca2+ and HCO₃-. Meanwhile, the surrounding metamorphic rocks limited the input of Na+. Geological origin was the dominant factor affecting the components of groundwater in this area. The TDS values in all water samples fell within the range of 100-1000 mg/L, which was consistent with the hydrochemical characteristics of groundwater in rock weathering-dominated regions [26]. This indicated that the major source of ions in the groundwater was the weathering and hydrolysis of rock minerals and that water-rock interaction played a dominant role in the formation and hydrochemical characteristics of shallow groundwater.

Ion correlation analysis can reflect the similarity between groundwater components and judge whether

the source of ions is consistent [27]. As shown in Table 3, the concentration of Ca²⁺ exhibited a significant positive correlation with HCO₃-, SO₄²-, and Cl⁻ (R>0.6, p<0.01), indicating that these ions shared a common source or formation process. HCO₃- showed a significant positive correlation with Mg2+ and Ca2+ (R = 0.74 and 0.601, p < 0.01). In addition, Ca^{2+} and SO₄²⁻, as well as Na⁺ and K⁺, show a positive correlation. TH is significantly positively correlated with Ca²⁺ (0.923**) and Mg²⁺ (0.838**), and there is also a highly significant correlation between TDS and TH (0.963**). As shown in Table 3, TDS exhibited a significant positive correlation with major cations (Ca2+, Mg2+, Na+) and anions (HCO₃-, SO₄²-, Cl-), with correlation coefficients R>0.6 (p<0.01). The positive correlation between Cl^- and NO_3^- (R = 0.515), along with the variations in the concentrations of SO₄²⁻, Cl⁻, and NO₃⁻, can reflect the impact of human activity pollution [28].

The formation of HCO₃⁻, Mg²⁺, and Ca²⁺ in the groundwater of the study area is, to some extent, influenced by the dissolution of minerals such as

Table 3. Conventional ion correlation analysis of shallow groundwater in the study area.

Parameters	TH	TDS	K ⁺	Ca ²⁺	Na ⁺	Mg ²⁺	HCO ₃ -	SO ₄ ²⁻	Cl-	NO ₃
TH	1									
TDS	0.963**	1								
K ⁺	0.396**	0.456**	1							
Ca ²⁺	0.923**	0.932**	0.290*	1						
Na ⁺	0.568**	0.694**	0.615**	0.565**	1					
Mg ²⁺	0.838**	0.745**	0.373**	0.564**	0.475**	1				
HCO ₃	0.748**	0.635**	0.212	0.601**	0.440**	0.740**	1			
SO ₄ ²⁻	0.691**	0.681**	0.377**	0.685**	0.607**	0.551**	0.587**	1		
Cl-	0.700**	0.768**	0.402**	0.695**	0.536**	0.525**	0.329*	0.314*	1	
NO ₃	0.117	0.304*	0.118	0.237	0.002	0.037	-0.317*	-0.257	0.515*	1

^{*}Correlation is significant at the 0.05 level (two-tailed)

^{**}Correlation is significant at the 0.01 level (two-tailed)

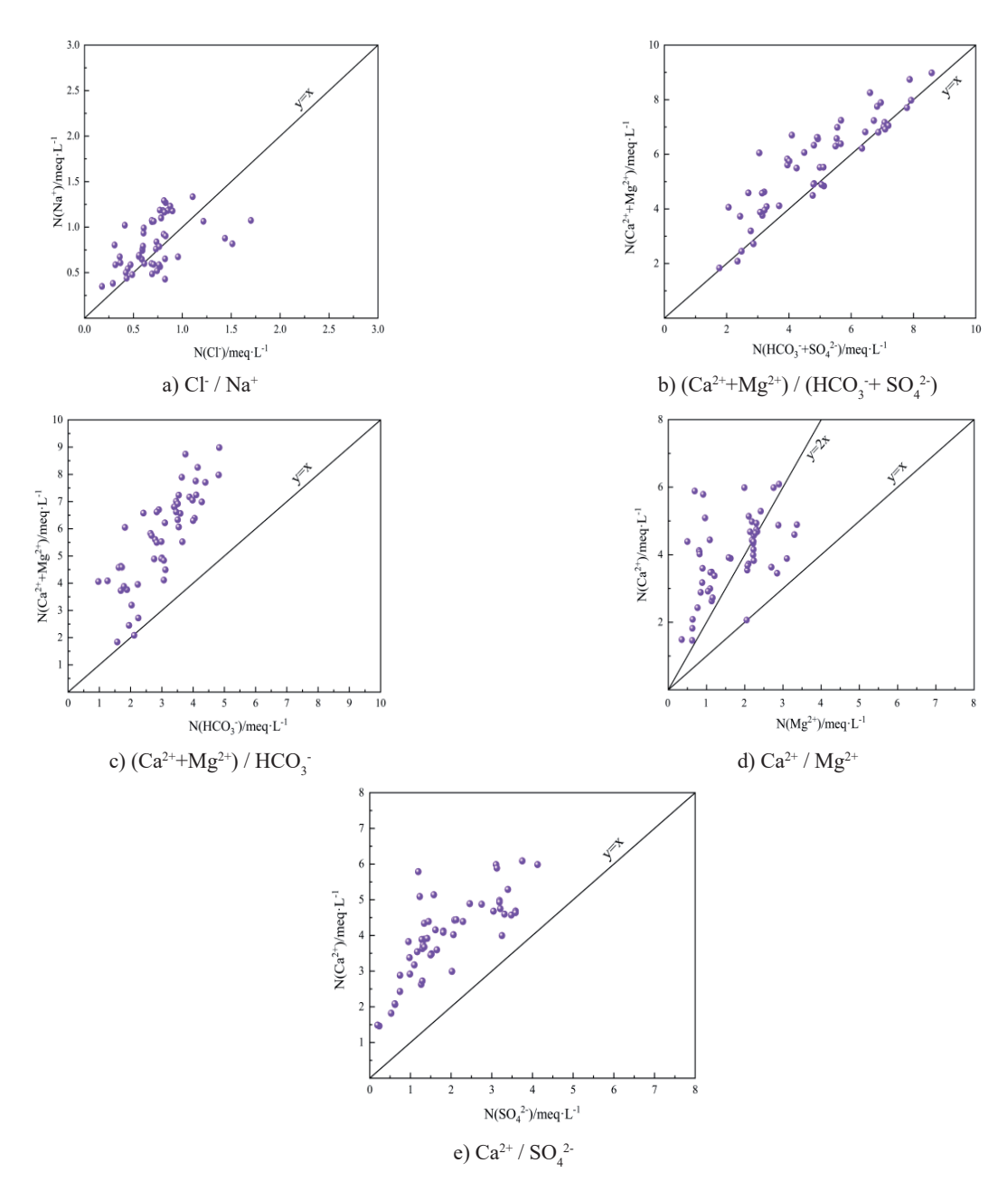


Fig. 5. Isovalue map of major ion ratios in groundwater.

dolomite and calcite, indicating that the dissolution process of carbonate rocks is the main factor affecting the hydrochemical characteristics of the groundwater. In particular, the significant positive correlation between Mg²⁺, Ca²⁺, TH, and TDS further supports this conclusion. The increase in TDS, along with the significant positive correlation with the aforementioned cations and anions, reflects the close relationship between the dissolved mineral content and TDS in the water.

The rocks exposed in the study area's strata contain trace to significant amounts of pyrite, and the positive correlation between Ca²⁺ and SO₄²⁻ suggests that frequent mining activities may have contributed large amounts of SO₄²⁻ and Ca²⁺ [29]. The positive correlation

between Na⁺ and K⁺ is related to the weathering of feldspar minerals in the Archaean strata. The K⁺ released during feldspar weathering and dissolution is easily adsorbed by clay minerals, leading to a weaker correlation with other ions.

To reveal the correlations between ionic variables, ion-ratio diagrams were plotted to further analyze the potential mineral sources of hydrochemical components and to better understand the origins of groundwater hydrochemistry [30]. As shown in Fig. 5a), the relationship between Cl⁻ and Na⁺ was mostly distributed near the 1:1 contour line, indicating that the main source of Na⁺ and Cl⁻ was the dissolution of salt rock minerals. When water samples were plotted above the N(Cl⁻/Na⁺) equiline, it indicated that, in addition to

the dissolution of halite, Na⁺ may also have been derived from cation exchange processes and the dissolution of sodium-bearing minerals such as feldspar [31]. This was particularly common in strata with active ion exchange capacity. In addition, a few data points were located below the equiline, with Cl⁻ concentrations slightly exceeding those of Na⁺, indicating that some areas may have been influenced by anthropogenic factors such as agricultural drainage or surface-water infiltration.

Fig. 5b), which plots N ($Ca^{2+} + Mg^{2+}$) / N ($HCO_3^- +$ SO₄²⁻), showed that most data points were distributed above the 1:1 equiline, indicating that Ca2+, Mg2+, HCO3-, and SO₄²⁻ primarily originated from the weathering and dissolution of carbonate minerals. The proximity of the data points to the equiline further suggested that the ions were mainly derived from the dissolution of both carbonate and evaporite rocks [32]. In the study area, dolomite and chert were the dominant lithologies, and the concentrations of Ca2+ and Mg2+ were mainly attributed to the weathering and dissolution of these carbonate rocks. The ratio N(Ca²⁺ + Mg²⁺)/N(HCO₃⁻) was used to further analyze the mineral sources of Ca^{2+} and Mg^{2+} . In the N ($Ca^{2+} + Mg^{2+}$)/N (HCO_3^-) plot (Fig. 5c)), all water samples were located above the 1:1 equiline, indicating that Ca2+ and Mg2+ were in excess relative to HCO₃-. This suggested that, in addition to carbonate weathering, the dissolution of silicate minerals (e.g., albite) also contributed to the presence of Ca2+ and Mg2+ in groundwater. If the reaction occurred under open system conditions, CO2 would be involved. In the study area, human activities may have led to the exposure of minerals and triggered oxidation reactions, during which CO₂ was preferentially consumed, thereby suppressing the formation of HCO₃⁻ [33]. In addition, wastewater irrigation in agricultural areas increased the concentrations of Ca²⁺ and Mg²⁺ in groundwater. A few water samples were located near the 1:1 equiline in the N (Ca²⁺ + Mg²⁺)/N (HCO₃⁻) plot, indicating that the dissolution of dolomite and limestone was the sole source of these ions.

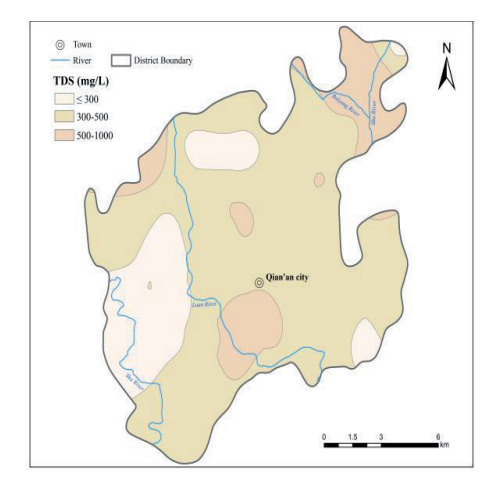
N(Ca²⁺)/N(Mg²⁺) served as an important indicator for identifying the sources of groundwater components. A ratio greater than 1 indicated that Ca²⁺ primarily originated from the dissolution of carbonate minerals, whereas a ratio less than 1 suggests that groundwater had greater contact with Mg-rich minerals such as dolomite, leading to elevated Mg²⁺ concentrations [34]. In the N(Ca²⁺)/N(Mg²⁺) plot (Fig. 5d)), the water sample points were relatively scattered, indicating a variety of mineral types and multiple ion sources in the study area. However, most of the samples clustered near the line y = 2x, suggesting that Ca^{2+} and Mg^{2+} in groundwater mainly originated from the dissolution of dolomite and limestone and that groundwater had undergone extensive interaction with carbonate minerals. A portion of the data points is plotted above the y = 2x line, implying that the dissolution of other minerals may have contributed to additional Ca²⁺. Further analysis based on the N (Ca^{2+})/N (SO_4^{2-}) plot (Fig. 5e)) showed that all data points were located above the 1:1 equiline, indicating Ca^{2+} enrichment or SO_4^{2-} depletion. This confirmed that the dissolution of carbonate rocks played a dominant role in the formation of groundwater hydrochemistry in the study area.

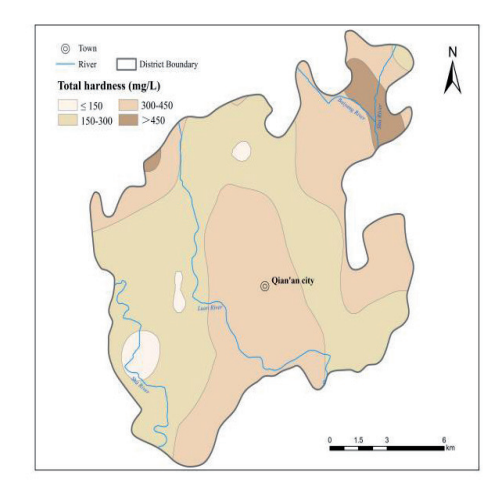
Spatial Distribution Characteristics of the Background Values

The environmental background value thresholds for TDS in groundwater in the study area were calculated to be 162-729.95 mg/L, with a mean value of 401.33 mg/L and a coefficient of variation of 33.66%; the TH background value thresholds ranged from 122.05 to 508.55 mg/L, with a mean value of 298.78 mg/L and a coefficient of variation of 32.37%, and there was some spatial variability in the distribution of both TDS and TH. The distribution of TDS and TH concentrations is shown in Fig. 6a) and 6b). Areas with TDS<300 mg/L and TH<150 mg/L were identified as low background value zones. The TDS in most areas of the study area was 300-500 mg/L, and the TH was 150-300 mg/L, indicating a medium background value zone. The highvalue zone of TH exceeding 300 mg/L was mainly distributed in the central part of the study area, the upper and lower reaches of the Luanhe River, and the northeastern region. These high-value areas largely overlapped with the zones of elevated TDS.

The variations in TDS and TH in groundwater were controlled and influenced by factors such as topography, lithology, burial conditions, and human activities. In areas with low background values, there are mountain uplifts with higher elevations. The groundwater flows from the northwest to the southeast, with abundant recharge from rainfall infiltration in the mountainous areas, resulting in a strong alternation in the groundwater cycle. Although the aquifer media experienced sufficient dissolution processes, the relatively steep hydraulic gradient promoted the rapid transport of dissolved cations, anions, and other chemical constituents toward the center of the study area along the flow path. As a result, the environmental background values of TDS and TH in this region remained relatively low.

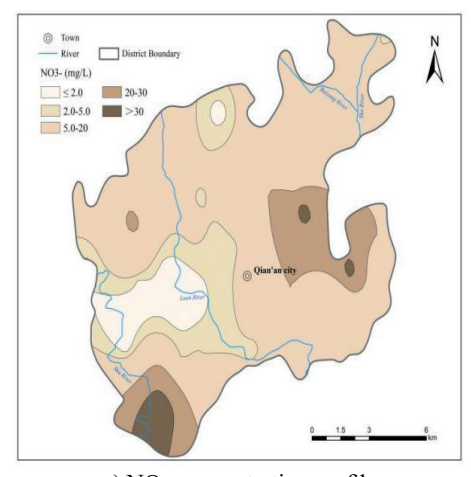
The surface water system in the study area was well developed, and the seepage recharge and runoff erosion from surface water bodies such as the Luanhe River and the Shahe River jointly influenced the hydrochemical characteristics of the groundwater. In the moderate background value area, runoff exerted scouring and erosional effects on carbonate rocks such as dolomite and limestone along its flow path, leading to the dissolution of large amounts of hydrochemical components such as Ca²⁺ and Mg²⁺ into the groundwater. Meanwhile, as groundwater from higher elevations converged toward the center of the study area, it carried dissolved constituents produced by earlier dissolution processes, which combined with existing solutes.





a) TDS concentration profile





c) NO₃ concentration profile

Fig. 6. Isovalue map of spatial concentration distribution for groundwater environmental background values.

This ultimately resulted in a rising trend in the regional background values of TDS and TH in the study area. This was highly consistent with the findings of Zhang et al. [35] in the Jinzi River Basin of Yunnan, China, where stable flow and low mineralization were observed in mountainous and hilly areas.

The center of the study area and the Luan River discharge area were high background value zones. The area has gentle terrain, and groundwater flow is slow. The infiltration capacity of the river decreases as the particle size of the sediment layers becomes finer. At the same time, as the groundwater depth decreases, the evaporation concentration effect is significantly enhanced, leading to an increase in the ion concentration of the groundwater. Urban, industrial, and agricultural water use disrupted the water-rock equilibrium: on one hand, groundwater extraction reduced the dilution capacity of the aquifer; on the other hand, anthropogenic activities increased pollutant inputs, to changes in the groundwater's acid-base environment

Due to the rapid economic and industrial development of Qian'an City, the average annual volume

of industrial groundwater over-extraction reached 35 million cubic meters [37]. Excessive extraction enhanced infiltration pathways, and some aquifers shifted toward a relatively oxidizing state. This transformation increased the solubility of certain calcium- and magnesium-bearing minerals, leading to greater concentrations of Ca²⁺ and Mg²⁺ in groundwater and, consequently, an increase in TH [38]. Anthropogenic activities, surface water infiltration, and strong evaporation collectively contributed to the rise in ion concentrations.

The environmental background value thresholds for NO₃ ranged from 0.002 to 32.62 mg/L with a coefficient of variation of 80.91%, indicating a highly uneven spatial distribution of NO₃ concentrations in the study area. This suggested that the background value of NO₃ was strongly influenced by anthropogenic activities. As shown in Fig. 6c), areas with high NO₃ concentrations (>20 mg/L) were primarily located along the lower reaches of the Xishahe River and the southeastern edge of the study area. The high-value zone in the west exhibited a banded distribution following the downstream course of the Xishahe River, while

the southeastern high-value area appeared in a scattered point-and-patch pattern. NO₃ concentrations across most of the study area ranged from 5.0 to 20 mg/L, and their spatial distribution largely coincided with urban settlements and agricultural land. This indicated that human activities were the primary contributors to elevated NO₃ levels in groundwater [39].

Iron ore deposits are found in the upstream of the Xisha River and around the high-value areas. The leachate from the waste rock piles generated by mining activities is the main source of groundwater contamination. The combined impacts of agricultural and mining activities intensified NO3 accumulation in the region. In particular, the widespread application of organic and chemical fertilizers in agriculture resulted in non-point source pollution, leading to the leaching of fertilizers, soil nitrogen, and livestock waste into the groundwater. Due to the low utilization efficiency of nitrogen fertilizers, a large proportion entered the aquifer through irrigation and rainfall infiltration [40]. In addition, the long-term and frequent extraction of groundwater for irrigation accelerated vertical groundwater flow, further contributing to the excessive accumulation of NO₃.

Conclusions

The pH of groundwater in the study area ranged from 6.6 to 8.5, with TDS values below 1 g/L and TH ranging from 92 to 851 mg/L. The dominant hydrochemical types were HCO₃-Ca·Mg and HCO₃·SO₄-Ca·Mg. Since TDS values were concentrated within the common range for shallow groundwater (100-1000 mg/L), the groundwater hydrochemistry was considered stable, and the dissolution of carbonate minerals mainly controlled ion concentrations. The Gibbs plot indicated that the primary source of groundwater ions in the study area was the weathering and hydrolysis of rock minerals, with water-rock interaction being the dominant controlling mechanism. Based on the ion correlation analysis and further analysis of the ratio diagrams, it was determined that the Ca²⁺, Mg²⁺, and HCO₃in the groundwater of the study area primarily originate from the dissolution of carbonate minerals. TH showed highly significant positive correlations with Ca^{2+} (0.923) and Mg^{2+} (0.838**). A similarly strong correlation was observed between TDS and TH (0.963**), indicating that as the concentrations of Mg²⁺, Ca²⁺, and other ions in the groundwater increased, total hardness increased, and the TDS concentration also increased accordingly. The changes in the concentrations of SO₄²⁻, Cl⁻, and NO₃⁻ indicated that human activities influenced the groundwater. Overall, the results suggested that geological factors remained the main influence on the hydrochemical composition of the groundwater.

Through calculation, the environmental background thresholds for TDS, TH, and NO, in the study area were

determined to be 162-729.95 mg/L, 122.05-508.55 mg/L, and 0.002-32.62 mg/L, respectively. The corresponding coefficients of variation were 33.66%, 32.37%, and 80.91%, indicating that TDS and TH exhibited a certain degree of spatial variability, while NO3 concentrations showed highly uneven spatial distribution and were strongly influenced by anthropogenic activities. The elevated background value of NO₃ was primarily caused by the influence of human activities. This paper only studied the spatial distribution characteristics and causes of the current situation of the background value of NO,, and the groundwater environment under the influence of human activities is still one of the future research directions. In response to the evolutionary trend of NO₃ in the study area, water quality data should be collected continuously, and long-term monitoring should be conducted at the boundary of the high background area.

Author Contributions

All authors contributed to the study conception and design. Xue Xia: Writing-Original Draft, Software, Funding Acquisition. Zhihui Qu: Writing-Review and Editing, Supervision, Funding Acquisition. Haowei Yuan: Investigation and Software. Zhiqiang Gong: Investigation. Sihui Shao: Investigation. Huimin Kong: Writing-Review. Biao Yu: Writing-Review and Editing, Funding Acquisition. All authors read and approved the final manuscript.

Acknowledgments

We sincerely thank the editor for their careful guidance during the review process, and we are grateful to the anonymous reviewers for their valuable comments and suggestions.

This research was supported by the Fundamental Research Funds for the Central Universities of China, grant number ZY20210304, and the Science and Technology Innovation Program for Postgraduate Students in IDP subsidized by Fundamental Research Funds for the Central Universities, grant numbers ZY20240307 and ZY20250312.

Conflict of Interests

The authors declare no conflict of interest.

Data Availability

Data cannot be made publicly available; readers should contact the corresponding author for details.

References

- CAI Z.Q., REN B.Z., XIE Q., DENG X.P., YIN W., CHEN L.Y. Toxic element characterization against a typical high geology background: Pollution enrichment, source tracking, spatial distribution, and ecological risk assessment. Environmental Research. 255, 119146, 2024.
- KIEU L.D., NGUYEN P.Q. Groundwater Quality Assessment in the Middle-Upper Pleistocene Aquifer. Civil Engineering Journal. 10 (7), 2357, 2024.
- 3. ZHANG Y.H., YAN Y.T., YAO R.W., WEI D.H., HUANG X., L M., WEI C.L., CHEN S., Y C. Natural background levels, source apportionment and health risks of potentially toxic elements in groundwater of highly urbanized area. Science of the Total Environment. 935, 173276, 2024.
- DENG Y.D., YE X.Y., DU X.Q. Progress and prospects of research on environmental background value of groundwater. China Environmental Science. 45 (5), 2530, 2024
- NAKIĆ Z., KOVAČ Z., PARLOV J., PERKOVIĆ D. Ambient background values of selected chemical substances in four groundwater bodies in the Pannonian region of Croatia. Water. 12 (10), 2671, 2020.
- HE B.N., HE J.T., SUN J.C., WANG J.J., WEN D.G., JING J.H., PENG C., ZHANG C.Y., Comprehensive Evaluation of Regional Groundwater Pollution: Research Status and Suggestions. Earth Science Frontiers. 29 (3), 51, 2022.
- KOUACOU B.A., ANORNU G., GIBRILLA A., ADIAFFI B., GYAMFI C. Hydrochemical evolution of groundwater in Soubré and Gagnoa counties, Côte d'Ivoire. Groundwater for Sustainable Development. 24, 101079, 2024.
- YAO R., ZHANG Y., YAN Y., WU X.C., UDDIN M.G., WEI D.H., HUANG X., TANG L.J. Natural background level, source apportionment and health risk assessment of potentially toxic elements in multi-layer aquifers of arid area in Northwest China. Journal of Hazardous Materials. 479, 135663, 2024.
- GAO Y.Y., QIAN H., HUO C.C., CHEN J., WANG H. Assessing natural background levels in shallow groundwater in a large semiarid drainage Basin. Journal of Hydrology. 584, 124638, 2020.
- LI X.Y., ZHANG Y.L., WANG L.J., SU R., LI Z.H. Study on Groundwater Environmental Background Values in Hetao Basin. Journal of Arid Land Resources and Environment. 34 (3), 180, 2020.
- BUSICO G., BORDBAR M., RUFINO F., SARRACINO A., TEDESCO D. Assessment of NO₃-, As, and F⁻ background levels in groundwater bodies: A methodological review and case study utilizing sequential Gaussian simulation (SGS). Groundwater for Sustainable Development. 26, 101211, 2024.
- 12. CHU Y.J., HE B.N., CHEN Z. HE J.T. Research on identifying the outliers of the TDS in shallow groundwater based on the random forest model. Earth. Science Frontiers. 32 (2), 456, 2025.
- AWAWDEH, A.R.M., YASARER H., GHAFFARI Z., YARBROUGH L.D. Downscaling GRACE Data for Improved Groundwater Forecasting Using Artificial Neural Networks. Civil Engineering Journal. 11, 406, 2025.
- 14. ZHU Y. Design of country parks in Semi-humid areas based on the goal of water security-Taking Zhaocun country park in Qian'anCity, Hebei Province as an example. Beijing Forestry University, 2022.

- 15. XU M., LU S., WEI W.G., YANG A.X., LIU H.L., AN M.Y., LI B. Geological and geochemical characteristics of deep and shallow orebodies in the Mengjiagou BIF iron deposit in the Qian'an area of the eastern Hebei, China and their geological significancs. Acta Mineralogica Sinica. 1, 2025.
- 16. WANG Y. Occurrence characteristics and pollution assessment of heavy metals on the surface of representative iron tailings ponds in Eastern Hebei Province. Liaoning Technical University, 2023.
- FENG Z.W. Spatial differentiation and visual expression of soilphysical and chemical characteristics in mining areas. North China University of Science and Technology, 2024.
- YANG X.F., LI Y.Q. Groundwater Resource Numerical Analysis and Evaluation by the Finite Element of the Qian'an Basin. Shanxi Architecture. (4), 130, 2008.
- 19. XU G.M., WU F., SHI Z.Y., BI P., LIU L.H., MA L.H. An Analysis of the Effect of Groundwater Regulation and Recovery in Groundwater Resources Areas near the Surface Water in the Qian'an Basin. China Rural Water and Hydropower. (8), 91, 2010.
- 20. MENG S.S. Research on groundwater environmental impact assessment of mining area on the west side of Luanhe River in Oian'an City. North China University of Science and Technology, 2022.
- 21. ZHANG W.R. Environmental evolution and coupling simulation of surface water and groundwater in Maguan River Basin driven by coal mining. Inner Mongolia Agricultural University, 2024.
- 22. LI Y.J., LI H.M., SU S.H., ZHANG C.X., LI M.D., ZHANG X.D. Effect of carbonate air carbonization on water salinization in a certain Reservoir. South-to-North Water Transfers and Water Science & Technology. 1, 2025.
- 23. LI X.M., WANG Y.J., JIA W.R., CHEN L.H., WU F.D. Geodiversity, Geoconservation and Sustainable Development in Qian'an National Geopark (Hebei, China). Geoheritage. 16 (3), 75, 2024.
- 24. YUAN J.Q., ZHAN D, BI Y.X., LI J., WEN S.M., BAI S.J. Acid mine drainage activation mechanism on lime-depressed pyrite flotation from copper sulfide ore. Transactions of Nonferrous Metals Society of China. 34 (9), 2987, 2024.
- SONG X.Q., PENG Q., WANG W., QU Q.N. Analysis of Environmental Background Values of Chloride and Sulfate in Shallow Groundwater in Karst Area of Guizhou. Earth Science. 44, (11), 3926, 2019.
- CHENG M., JIANG J.Y., REN J., ZHAO Z.H. Groundwater Hydrochemical Characteristics and Groundwater Quality Evaluation in Qapqal County Area. Science Technology and Engineering. 20 (2), 527, 2020.
- 27. FANG L.J., GAO R.Z., JIA D.B., YU R.H., LIU X.Y., LIU T.X. Spatial-Temporal Characteristics of Groundwater Quality and Its Environmental Driving Factors of Steppe Basin—Taken Balaguer River Basin of Inner Mongolia for Instance. China Environmental Science. 41 (5), 2161, 2021.
- LIU Z., PAN H.Y. Preliminary Study on Groundwater Environmental Background Value in Plain Area of Hubei Province. Safety and Environmental Engineering. 30 (3), 208, 2023.
- 29. LINGHU C.W., ZOU S.L., GUAN J.Y., CHAI C., YANG L.L., HE C.Z., ZHU P.P., CUN D.X., LIU Z.L., ZHU X.Q., XU L. Hydrochemical characteristics and quality assessment of groundwater in typical coal mining areas of Fuyuan, EasternYunnan. Geology in China. 1, 2025.

- 30. LU W.G., JIANG Y.W., MA X.Y., LIU L., XUE J., ZHANG B., HUANG C.B. Chemical Characteristics of Surface Water and Groundwater in Plain Area of the Qargan River Basin on the North Slope of Kunlun Mountains. Arid Land Geography. 47 (10), 1617, 2024.
- WEI Z.L., JI Y., LI Y., FANG H.M., DONG D.L., YU L.J. An Analysis of Multi-Coal Seam Mining Impacting Aquifer Water Based on Self-Organizational Maps. Water. 17 (4), 598, 2025.
- 32. DING Q.Z., LEI M., ZHOU J.L., ZHANG J., XU D.S. An Assessment of Groundwater, Surface Water, and Hydrochemical Characteristics in the Upper Valley of the Bortala River. Arid Zone Research. 39 (3), 829, 2022.
- KLAUS M. Decadal increase in groundwater inorganic carbon concentrations across Sweden. Communications Earth and Environment. 4, 221, 2023.
- 34. XU J.Z. Environmental hydrogeochemical characteristies of groundwater in Loose Bed of the Huaibei Plain. University of Science and Technology of China, 2024.
- 35. ZHANG X.C., ZHANG Y.C., GUI Y.J., SUN R.Y., LI J., WU Q., DING Y.K., CHEN K. Chemical characteristics of groundwater and surface water affected by human activities in the upper Jinzi River Basin, China. Scientific Reports. 15, 9294, 2025.
- 36. CAO B., TANG P.J., JIAO Y.F., GUO Y.P., LIN H.X., WANG G. An Analysis of Hydro-chemical

- Ccharacteristics of Groundwater in Over-exploited Area of Northern Weifang. China Rural Water and Hydropower. (3), 85, 2017.
- 37. ZOU J.D., CAI H.W., XIA C.X., FU J., GONG Y.Z., WANG J.X., ZHOU F. Quantification of sector-specific groundwater withdrawals considering water diversion projects in the Hebei Province, China. Journal of Hydrology: Regional Studies. 55, 101923, 2024.
- 38. PAPPALARDO G., BORSI I., ROSSETTO R., TRANCHINA G., BONGIOVANN M., FARINA M., MINEO S. Unravelling the influence of heterogeneities and abstraction on groundwater flow and solute transport in a fractured carbonate aquifer, Sicily, Italy. Hydrogeol Journal. 32, 1071, 2024.
- 39. DING K., ZHANG Y., ZHANG H., YU C., LI X., ZHANG M., ZHANG Z., YANG Y. Tracing nitrate origins and transformation processes in groundwater of the Hohhot Basin's Piedmont strong runoff zone through dual isotopes and hydro-chemical analysis. Science of the Total Environment. 919, 170799, 2024.
- 40. GE D., GAO X.D., JIANG P.Y., LI B., HE N.N., WU Y.B., HE Q.H., CAI Y.H., LI C.J., ZHAO X.N. Deep soil desiccation hinders nitrate leaching to groundwater in the global largest apple cultivation area. Journal of Hydrology. 637, 131334, 2024.